17th Australasian Fluid Mechanics Conference
Auckland, New Zealand
5-9 December 2010

Fluid-Structure Interaction of Gas Turbine Blades

P. Dhopade[1], A.J. Neely[1] and J. Young[1]

[1]School of Engineering and Information Technology
University of New South Wales at the Australian Defence Force Academy,
Canberra, Australia Capital Territory 2600, Australia

Abstract

This study investigates the effects of low-cycle and high-cycle fatigue interaction on the aerodynamic and structural behaviour of a fan blade. A numerically based analysis through the interfacing of computational fluid dynamics (CFD) and finite element modelling (FEM) analysis, referred to as fluid-structure interaction (FSI) is performed. This paper reports initial results from an ongoing study on numerical simulations of two-way FSI to predict representative fluctuating loads on the fan rotor blades of the first axial compressor stage of a representative gas turbine engine. The stator blade is modelled upstream of the rotor blades to simulate the turbulent shedding of wakes that result in aerodynamically induced vibrations of the rotor blades, a leading cause of high-cycle fatigue. The rotor blades are also subject to low-cycle fatigue induced by both the high rotational loads and the mean aerodynamic pressure loading experienced by the blades at various operating conditions. The results demonstrate that the presence of the upstream stator results in an increased aerodynamic load on the rotor blades when compared to the case where the upstream stator is absent. This implies that the presence of the upstream stator must be included in the FSI numerical model to fully predict the complex interaction between high-cycle fatigue and low-cycle fatigue.

Introduction

Fatigue due to repeated fluctuating loads is a major cause of damage and failure of gas turbine engine components, which are subject to both low-cycle fatigue (LCF) and high-cycle fatigue (HCF) loads during operation. To improve engine reliability, durability, and maintainability through improved engine structural integrity, it is necessary to understand the interaction of LCF and HCF in these components, which can have a direct effect on the overall life of the engine and its components.

Low-Cycle Fatigue and High-Cycle Fatigue

The LCF loads are a result of the aircraft flight profile and are typically high stress, as shown in figure 1. The fan rotor blades of the compressor first stage considered here are thus subject to aerodynamic and rotational loads, while thermal loads are neglected because the temperature in the compressor is considerably less in comparison to turbine temperatures.

HCF loads are a consequence of vibrating components at high frequencies, for e.g., fluctuating loads on compressor blades as they rotate through the wakes generated by the upstream stator vanes. HCF loading on rotating blades is the leading source of engine component failure. The effect of this loading can be investigated by accurately predicting the HCF loads caused by turbulent flow-induced vibration of rotating engine components at engine operating conditions [5].

Other contributors to HCF loads are mechanical vibration, acoustic fatigue and airfoil flutter, which for the sake of simplicity, are omitted from this study. The combined effect of LCF and HCF results in a significant reduction to the fatigue life of the blades [5].

It has been found that the resulting fatigue behaviour of joint HCF and LCF loading is not the linear summation of the individual fatigue produced by the loadings occurring sequentially [9], suggesting the occurrence of a coupled interaction between the fluid and structure.

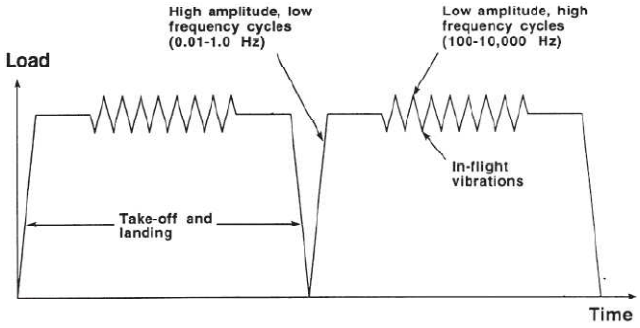

Figure 1. Schematic of simplified engine mission spectrum [8].

Fluid-Structure Interaction

Fluid-structure interaction (FSI) is the coupling effect of structural deformation on fluid flow. It has been established that HCF induced fatigue of the rotor blade is highly influenced by the wake passing of the upstream stator vanes [5]. The flow field is further complicated by the presence of oscillating shocks and strong flow separation [4]. The resulting unsteady aerodynamic loading can result in a coupled FSI.

Recent developments in commercial software have largely automated the FSI process, rendering it a more attractive tool for the investigation of flow based problems, including the use of a two-way FSI analysis, in which coupling data is transferred at fluid-solid interfaces in an iterative process to solve the equation sets for all fields. A number of researchers have used FSI to investigate blade aeroelastic behaviour [4], optimize blade design parameters based on fatigue life estimates [7] and also advance the algorithms used for computational accuracy [11].

The purpose of this initial study is to implement the FSI methodology to investigate the importance of the upstream stator while demonstrating the effects of HCF induced vibration on the rotor blades due to the wake passing of the upstream stator vanes. Hence, two models are analysed separately, where the rotor blades are subjected to the absence and presence of the upstream stator vanes.

Model Description

A transonic compressor fan first stage rotor comprising of 32 blades is considered with the presence of 18 upstream stator vanes, as shown in figure 2(a).

However, since the computational time required to fully resolve the FSI for the complete annulus of the compressor is too large, the model has been reduced to one rotor blade for the case without the stator vanes, while one stator vane and two adjacent rotor blades are used for the second model, as depicted in figure 2(b).

A reduced model is valid due to the cyclic periodicity of steady and unsteady flows in turbomachinery. Thus, it is possible to analyse one or two blades with the implementation of appropriate periodic boundary conditions on the blade passages [2].

For this study, the fan rotor blades were subjected to a rotational speed of 11000 RPM and fan inlet conditions, which includes a free stream flow speed of 132 m/s at the fan face, at an altitude of 35000 ft (10668 m).

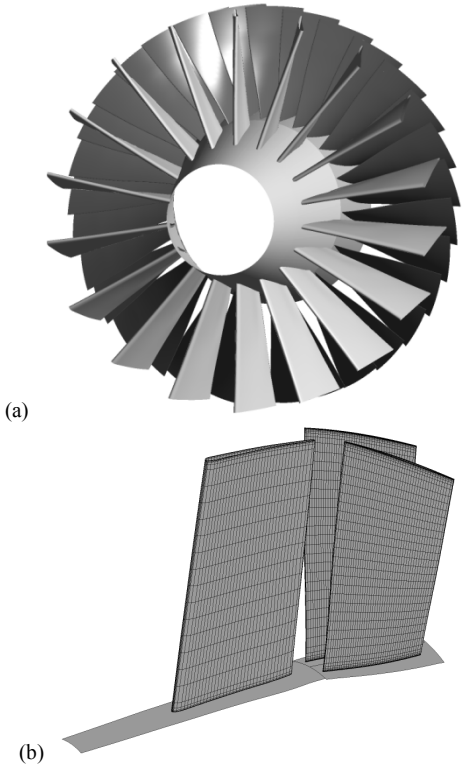

Figure 2(a). Full model of transonic compressor fan, (b) reduced model with one upstream stator vane and two adjacent rotor blades.

Numerical Method

The unsteady Navier–Stokes equations are discretized and solved iteratively using the finite volume technique:

$$\frac{\partial \rho}{\partial t} + \nabla \cdot (\rho \boldsymbol{U}) = 0 \qquad (1)$$

$$\frac{\partial (\rho \boldsymbol{U})}{\partial t} + \nabla \cdot (\rho \boldsymbol{U} \times \boldsymbol{U}) = -\nabla p + \nabla \cdot \tau + \boldsymbol{S}_M \qquad (2)$$

where the stress tensor, τ, is related to the strain rate by

$$\tau = \mu \left(\nabla \boldsymbol{U} + (\nabla \boldsymbol{U})^T - \frac{2}{3} \delta \nabla \cdot \boldsymbol{U} \right) \qquad (3)$$

The total energy equation is solved to account for heat transfer in the flow:

$$\frac{\partial (\rho h_{tot})}{\partial t} - \frac{\partial p}{\partial t} + \nabla \cdot (\rho \boldsymbol{U} h_{tot}) = \nabla \cdot (\lambda \nabla T) + \nabla \cdot (\boldsymbol{U} \cdot \tau) + \boldsymbol{U} \cdot \boldsymbol{S}_M + \boldsymbol{S}_E \qquad (4)$$

Where h_{tot} is the total enthalpy, related to the static enthalpy, h, by $h_{tot} = h + \frac{1}{2}\boldsymbol{U}^2$. The term $\nabla \cdot (\boldsymbol{U} \cdot \tau)$ indicates the work done due to viscous stresses, while the term $\boldsymbol{U} \cdot \boldsymbol{S}_M$ represents the work done due to external momentum sources and is neglected by the solver in this case.

The three-dimensional mesh for both models is constructed of approximately $6(10^5)$ quadrilateral elements as seen in figure 2(b) (structural domain) and figure 3 (fluid domain). A no-slip boundary condition is imposed on the blade surface and blade hub, while rotational periodicity is used for the blade passage.

The Shear Stress Transport (SST) turbulence model, which uses a combination of the two-equation models *k-ε* and *k-ω*, is employed due to its accuracy in predicting complex turbulent flows and its ability to resolve strong pressure gradients and separated flows experienced by axial compressors, as validated with experimental data by [1] and [13]. The boundary layer seen in figure 3 is resolved to ensure a near-wall y+ of less than 1 to comply with wall function constraints.

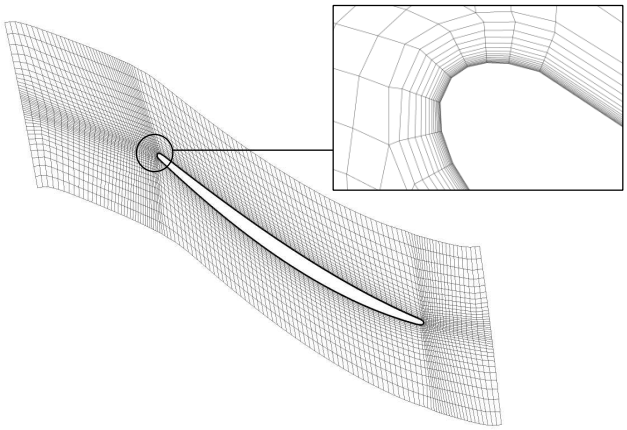

Figure 3. Quadrilateral elements used for rotor blade at midspan and growth of boundary layer elements.

In this quasi-static two-way FSI analysis, the results of the structural analysis are transferred to the fluid solver as a displacement boundary condition on the fluid-structure mesh interface. Similarly, the results of the fluid solver are passed back to the structural solver as a pressure load. The analyses continue until overall equilibrium is reached between the fluid and structural solvers. For the model with the isolated rotor, the FSI required 4000 iterations for both solvers to converge, while the model with the upstream stator required 10000 iterations, both at a timestep of 10^{-7} seconds.

Results

Model with no upstream stator vanes

The flow field around the rotating blade in the absence of the upstream stator vane results in the flow field shown in figure 4, the local Mach number relative to the blade is supersonic everywhere except the leading edge tip, where a bow shock wave is visible and at the trailing edge tip, where a strong wake and trailing edge shock waves are visible, validated by previous experimental results of transonic turbomachinery flows presented in [12].

The Mach number is supersonic around the blade due to the high rotational velocity of the rotor in addition to the subsonic axial velocity of the compressor, resulting in a Mach number of 1.4 at the rotor stage inlet.

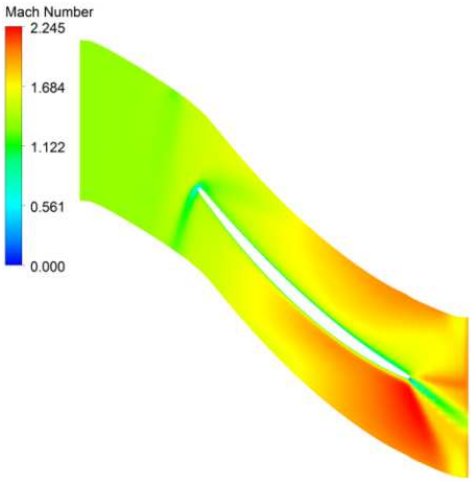

Figure 4. Mach number flow field around rotor blade at midspan in absence of stator vane.

Figure 5 shows the static pressure field around the blade at half-span, once again highlighting the leading edge bow shock wave, including the stagnation point in addition to the trailing edge shock waves.

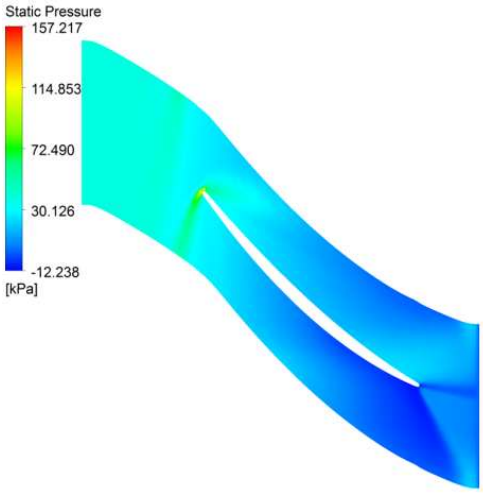

Figure 5. Static pressure flow field around rotor blade at midspan in absence of stator vane.

Figure 6(a) shows the static pressure loading on the blade suction surface, where the maximum pressure is not visible because it occurs on the leading edge of the blade. Note that the suction surface is defined as the convex surface of the blade, or the bottom surface of the blade profiles in figures 4 and 5. Since the region of high pressure occurs at the blade leading edge tip and decreases radially along the span, as expected for a transonic fan blade, the results are comparable to the surface static pressure field shown in [6].

The structural response of the blade can be seen in figure 6(b), which reflects the strain field. The elastic strain is greatest at the leading edge root since it is known that the cantilevered blade experiences a maximum load and corresponding deflection at the tip, also referred to as the first bending mode in an aeroelastic context [3,10].

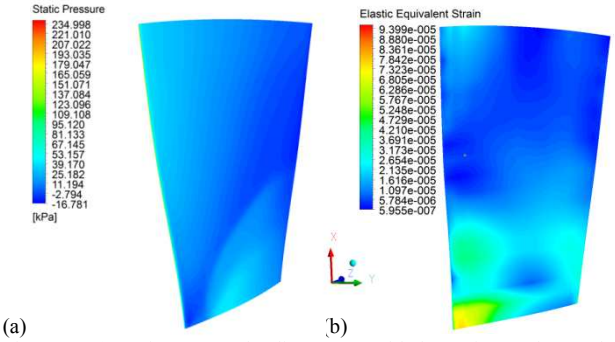

(a) (b)

Figure 6. (a) Static pressure loading on rotor blade suction surface and, (b) Elastic strain of rotor blade in absence of stator vane. Axial direction is along z-axis.

Model with one upstream stator vane

Figures 8 and 9 show similar flow fields for the adjacent rotor blades in the presence of the upstream stator vane. The flow along the stator vane is reasonably uniform, except at the leading edge stagnation point and trailing edge wake. The Mach number goes from subsonic to supersonic as the flow transitions from a stationary to rotational frame and the high rotational speed of the rotor. The upstream flow around the stator as experienced by the rotor blades is assumed to be steady for this quasi-static analysis. Similar to the first model in figure 4, there is a bow shock wave at the leading edge and oblique shock waves at the trailing edge of the rotor, also confirmed by the static pressure field in figure 9.

Figure 10(a) shows the static pressure loading on the blade suction surfaces of the rotor blades. The loading is similar to that of the isolated rotor model in figure 6(a); however the static pressure in the leading edge tip region is higher than that of the rotor with no upstream stator vane.

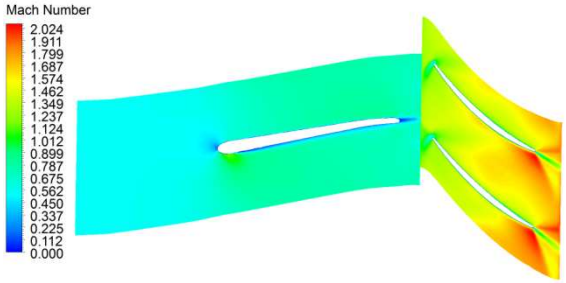

Figure 8. Mach number flow field around rotor blade at midspan in presence of stator vane.

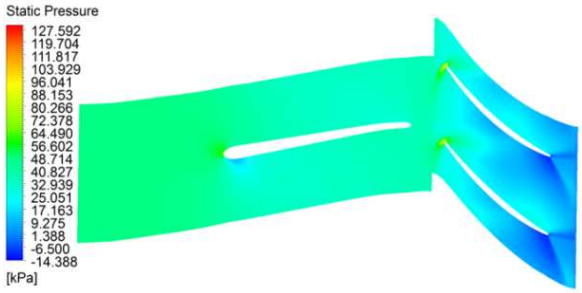

Figure 9. Static pressure flow field around rotor blade at midspan in presence of stator vane.

Figure 10(b) shows the elastic strain for the case with upstream stators. The strain field is similar to that of the isolated rotor in figure 6(b) with the maximum strain occurring at the leading

edge root. The magnitude of strain is also similar to that of the isolated rotor case, implying an equivalent range of deflection. A higher strain at the leading edge tip of the blade in both cases suggests twisting of the blade. A transient structural modal analysis would shed insight onto the vibrational response of the blades as they deform in the time domain [14].

This is apparent from figure 11, where the static pressure distribution is plotted at fullspan on the pressure and suction surfaces of the rotor blades, from leading edge to trailing edge, indicated by the streamwise location (0 is at the leading edge and 1 is at the trailing edge). The model with the upstream stator vane experiences a higher static pressure across the entire blade, when compared to the model in the absence of an upstream stator vane. This signifies that the wake passing due to the upstream stator vane increases the fluctuating aerodynamic load on the rotor blades, especially at the leading edge.

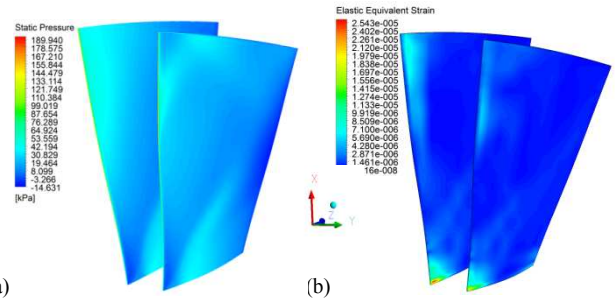

(a) (b)

Figure 10. (a) Static pressure loading on rotor blade suction surface and (b) Elastic strain of rotor blade in presence of stator vane. Axial direction is along z-axis.

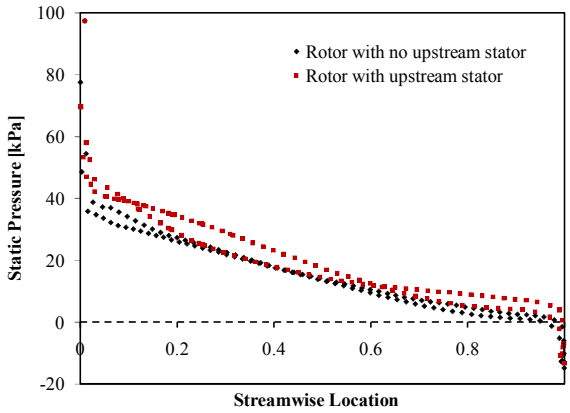

Figure 11. Static pressure distribution at fullspan for both models from leading edge to trailing edge of rotor blades. (Note that the pressure peak at the leading edge has been cropped).

Conclusions

Fluid-structure interaction has been demonstrated as a technique to investigate the effect of LCF and HCF interaction on the blades of a transonic rotor. Two models were analysed, one with the presence of the upstream stator vane and one without. The flow is supersonic over the rotor blades, causing shock waves at the leading and trailing edges. It is evident that the HCF loads due to the wake passings of the upstream stator vanes increase the aerodynamic pressure loads on the rotor blades, thus having a direct effect on their fatigue life. It is thus important to account for the effect of upstream stators in the FSI analysis to better estimate the overall life of the rotor blades. In terms of future research, it will be beneficial to use the load spectrum resulting from a transient fluid-structure interaction of the rotor blades to conduct a fatigue analysis using a damage tolerant approach [4], in order to estimate the reduction in fatigue life of the blades. The implications of this research can influence future experimental studies that aim to generate meaningful fatigue data, which will assist in the management of safe operation of these engines.

Acknowledgments

The Defence Science and Technology Organisation (DSTO) and the Defence & Security Applications Research Centre (DSARC) are gratefully acknowledged for supporting the author's research and participation in the conference.

References

[1] Balasubramanian, R., Barrows, S. & Chen, J., "Investigation of Shear-Stress Transport Turbulence Model for Turbomachinery Applications," presented at the 46th AIAA Aerospace Sciences Meeting and Exhibit, Reno, Nevada, 2008.

[2] Campobasso, M.S. & Giles, M.B., "Stabilization of linear flow solver for turbomachinery aeroelasticity using recursive projection method," *AIAA Journal,* vol. 42, pp. 1765-1774, 2004.

[3] Carstens, V., Kemme, R. & Schmitt, S., "Coupled simulation of flow-structure interaction in turbomachinery," *Aerospace Science and Technology,* vol. 7, pp. 298-306, 2003.

[4] Corran, R.S.J. & Williams, S.J., "Lifing methods and safety criteria in aero gas turbines," *Engineering Failure Analysis,* vol. 14, pp. 518-528, 2007.

[5] Cowles, B.A., "High cycle fatigue in aircraft gas turbines - an industry perspective," *International Journal of Fracture,* pp. 147-163, 1996.

[6] Cumpsty, N.A., "Current Aerodynamic Issues for Aircraft Engines," *Eleventh Australasian Fluid Mechanics Conference, Vols 1 and 2,* pp. 799-811, 1992.

[7] Lau, Y.L., Leung, R.C.K. & So, R.M.C., "Vortex-induced vibration effect on fatigue life estimate of turbine blades," *Journal of Sound and Vibration,* vol. 307, pp. 698-719, 2007.

[8] Nicholas, T., "Critical issues in high cycle fatigue," *International Journal of Fatigue,* vol. 21, pp. S221-S231, 1999.

[9] Powell, B.E., Hawkyard, M. & Grabowski, L., "The growth of cracks in Ti-6Al-4V plate under combined high and low cycle fatigue.," *International Journal of Fatigue,* vol. 19, pp. 167-176, 1997.

[10] Sadeghi, M. and Lui, F., "Coupled fluid-structure simulation for turbomachinery blade rows," in 43rd AIAA, Aerospace Sciences Meeting and Exhibit, 2005.

[11] Voigt, C., Frey, C. & Kersken, H., "Development of a generic surface mapping algorithm for fluid-structure-interaction simulations in turbomachinery," presented at the V European Conference on Computational Fluid Dynamics, Lisbon, Portugal, 2010.

[12] Wernet, M. P., "Application of dpiv to study both steady state and transient turbomachinery flows," Optics & Laser Technology, vol. 32, no. 7-8, pp. 497–525, 2000

[13] Yin, S., Jin, D.H., Gui, X.M., & Zhu, F., "Application and Comparison of SST Model in Numerical Simulation of the Axial Compressors," *Journal of Thermal Science,* vol. 19, pp. 300-309, 2010.

[14] Zhou, X. and Wolff, J., "Transonic compressor IGV/rotor interaction analysis including fluid structure interaction," in 22nd Applied Aerodynamics Conference and Exhibit, 2004.